Contents lists available at YXpublications

International Journal of Applied Mathematics in Control Engineering

Journal homepage: http://www.yxpublications.com/ijamce/index.html

Research on Performance of Switched Reluctance Motor based on Structural Parameters

Ye Rong[a,*], Qingyi Kong[a,b], Wenda Qi[a], Chao Li[a], Huan Wu[a]

[a] *Hebei Jiaotong Vocational and Technical College, Shijiazhuang 050035 ,China.*

[b] *Army Engineering University of PLA (Shijiazhuang) , Shijiazhuang 050000 ,China.*

ARTICLE INFO

Article history:
Received 12 April 2019
Accepted 15 June 2019
Available online 10 October 2019

Keywords:
Switched reluctance motor
Structural parameters
Motor performance

ABSTRACT

In this paper, the experimental study is carried out on two kinds of switched reluctance motor with the same power of the four phase 8/6 pole and four phase 16/12 pole with the same rated parameters. Electromagnetic simulation analysis of self-inductance, mutual inductance, torque and pulsation effect and winding current of two different SRM windings is carried out. The results show that compared with 16/12 pole, 8/6 pole switched reluctance motor has large self-inductance value, large mutual inductance value, large torque, small torque ripple, small current and good performance. This research has important guiding significance for the design of SRM motor body.

1. Introduction

Switched reluctance motor (SRM), as a new control motor, has developed rapidly in recent years. Its simple structure, low cost, high reliability and excellent speed regulation and start-up performance have been widely used in many fields, such as aerospace, compressor and electric vehicle [1-3]. However, due to the double salient structure of SRM itself, there is a large torque ripple during the operation of the motor, which causes excessive noise, noise pollution and power loss [4]. Therefore, what measures should be taken to solve the problem of excessive torque ripple has become an urgent problem to be solved. In the past, the problem of torque ripple is analyzed from the control strategy. The change of motor structure parameters will also cause the change of motor performance and torque ripple. This paper will analyze the influence of motor parameters on motor performance through simulation experiments.

2. Numerical approach

On the premise of determining the basic performance of the motor, such as rated voltage, output power and speed, what kind of structure should be adopted in the motor to achieve the best performance? At present, there is little research on the structure of the internal motor of switched reluctance, and the internal design has not yet formed a unified standard.

There are four main types of SRM motors used in the field of electric vehicles. They are three-phase 6/4 pole, three-phase 12/8 pole, four-phase 8/6 pole, four-phase 16/12 pole [6-9], Wang Mianhua [10] and so on. The comparative analysis of three-phase 6/4 pole switched reluctance motor speed regulation system (SRD) and four-phase 8/6 pole SRD shows that they can be used for both purposes. Motor or generator, it is more advantageous to develop and apply three-phase 6/4 pole switched reluctance motor in order to improve the unit volume capacity and system efficiency of motor. The above research is aimed at the motor structure with different phases. At present, there is no relevant research on the switched reluctance motor with different phases[11-13]. In this paper, four-phase 8/6-pole and four-phase 16/12-pole SRM motors are selected for simulation analysis, and the influence of structural parameters on the performance parameters of SRM motors is analyzed.

The main factors affecting the operation characteristics of SRM are the phase current waveform, the position of the rotor when the peak current and peak current appear[14-15]. However, the winding current of switched reluctance motor is neither DC constant nor alternating sinusoidal value in actual operation, and there is no rule to follow with the change of motor running time, which brings great difficulties to phase current analysis. Similarly, the electromagnetic relationship is also difficult to determine. In order to clarify the basic electromagnetic relationship and basic characteristics of the motor, the mathematical model of winding inductance, winding current, winding flux and torque is established.

2.1 Winding inductance

The relationship between inductance and rotor position angle can

* Corresponding author.
E-mail addresses: lele-9999@163.com (Y. Rong)

be expressed by functional relation.

$$L_{\min}=\begin{cases} L_{\min} & (\theta_1\le\theta<\theta_2)\\ L_{\min}+K(\theta-\theta_2) & (\theta_2\le\theta<\theta_3)\\ L_{\max} & (\theta_3\le\theta<\theta_4)\\ L_{\max}-K(\theta-\theta_4) & (\theta_4\le\theta<\theta_5)\end{cases} \tag{1}$$

$$\mathrm{K}=\frac{\mathrm{L}_{\max}-\mathrm{L}_{\min}}{\theta_3-\theta_2}=\frac{\mathrm{L}_{\max}-\mathrm{L}_{\min}}{\beta_s} \tag{2}$$

where L and θ Indicate inductance and rotor position angle respectively, and K and β_s indicate inductance change rate and stator pole arc respectively.

2.2 Winding flux linkage

The relationship between flux linkage ψ(θ)and rotor position angle θ can be expressed as a function.

$$\psi(\theta)=\begin{cases} \frac{\mathrm{U_s}}{\omega_r}(\theta-\theta_{on}) & (\theta_{on}\le\theta<\theta_{off})\\ \frac{\mathrm{U_s}}{\omega_r}(2\theta_{off}-\theta_{on}-\theta) & (\theta_{on}\le\theta<\theta_{off})\\ 0 & (others)\end{cases} \tag{3}$$

2.3 Winding current

Since the expression of winding inductance is piecewise linear, it is necessary to give initial conditions to solve winding current in stages.

$$\mathrm{i}(\theta)=\begin{cases} \frac{\mathrm{U_s}}{\omega_r}\frac{\theta-\theta_{on}}{\mathrm{L_{min}}} & (\theta_1\le\theta<\theta)\\ \frac{\mathrm{U_s}}{\omega_r}\frac{\theta-\theta_{on}}{\mathrm{L_{min}}+K(\theta-\theta_1)} & (\theta_2\le\theta<\theta_{off})\\ \frac{\mathrm{U_s}}{\omega_r}\frac{2\theta_{off}-\theta_{on}-\theta}{\mathrm{L_{min}}+\mathrm{K}(\theta-\theta_2)} & (\theta_{off}\le\theta<\theta_3)\\ \frac{\mathrm{U_s}}{\omega_r}\frac{2\theta_{off}-\theta_{on}-\theta}{\mathrm{L_{max}}} & (\theta_3\le\theta<\theta_4)\end{cases} \tag{4}$$

2.4 Electromagnetic torque

Inductance expressions at different locations can be derived and substituted.

$$\mathrm{T_e}=\begin{cases} 0 & (\theta_1\le\theta<\theta_2)\\ 0.5\mathrm{Ki}^2 & (\theta_2\le\theta<\theta_3)\\ 0 & (\theta_3\le\theta<\theta_4)\\ -0.5\mathrm{Ki}^2 & (\theta_4\le\theta<\theta_5)\end{cases} \tag{5}$$

3. Parameters and simulation of motor

In order to make a better comparative analysis, the structural parameters of the two motors are basically the same. The difference lies only in the different poles of the stator and rotor inside the motor. Two kinds of motors are designed, including 8/6 pole motor with 8 poles of stator, 6 poles of rotor, 16/12 pole motor with 16 poles of stator and 12 poles of rotor.

Tab.1 Two main parameters of SRM

parameters / structure	8/6poles	16/12poles
P/kW	5	5
U/V	72	72
n/（r/min）	6100	6100
Stator outer diameter/mm	155	155
Rotor outer diameter/mm	85	86
tooth width/mm	14.09	6.59
Rotor tooth width/mm	18.54	9.21
Core stacking/mm	102	102
First air gap/mm	0.4	0.4
Axle diameter	32	32

Two kinds of motors are modeled and simulated by Ansoft electromagnetic simulation software. The structure sketch is shown in Fig. 1.

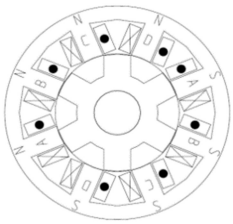

(a) 8/6 poles

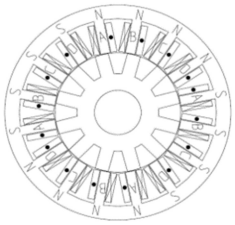

(b) 16/12 poles

Fig.1 Four-phase 8/6 pole structure and four-phase 16/12 pole structure

4. Modeling and parameter setting

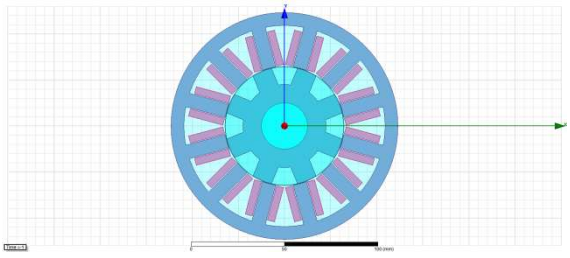

Fig.2 Maxwell 2D Motor Model

The RMxprt module has the function of deriving two-dimensional model. The two-dimensional simulation model is directly derived from the model already created in the RMxprt module. The derived model is shown in Figure 2.

At the same time of generating the two-dimensional model, the power conversion circuit accompanying the generation of the excitation source is shown in Fig. 4-12. Two voltage sources, V23 and V24, each 36V, constitute an excitation voltage of 72V.

D31-D36 diode and S_37-S_42 switching device constitute three power switching devices to control the on-off of the winding. D25-D30 is a continuous current diode, LPhaseA, LPhaseB, LPhaseC are three-phase windings, RA, RB, RC are equivalent resistance of the winding, LA, LB, LC are equivalent inductance of the winding, V14, V15, V16 are pulse control signals. To control the switching device on and off. This simple control circuit is used to realize the simulation of switched reluctance motor.

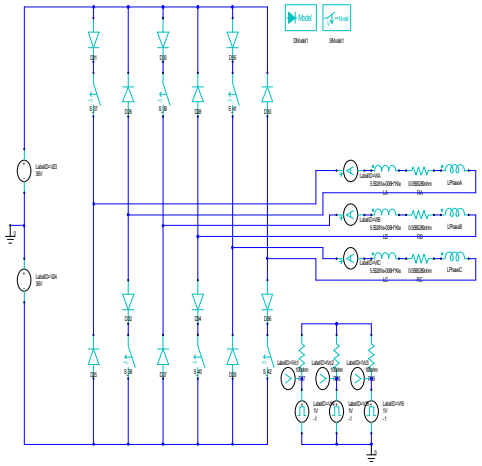

Fig.3 Power Conversion Circuit

In Maxwell 2D simulation, the magnetic line distribution of the motor can be obtained, as shown in Figure 4. The condition of the magnetic line shown in the figure is that the phase A winding is turned on, the time is 0.4 ms, the speed is 6136.82rpm, and the position angle is 29.75 deg. The magnetic line loops and distribution can be clearly seen in the figure. In the loop of the magnetic line, the magnetic line in the air gap is in a bending state, because the flux always closes along the path with the smallest reluctance, so a magnetic force will be generated to rotate the rotor counterclockwise, so that the salient poles of the stator and rotor are aligned until they are fully aligned. The magnetic line is not bent, and no magnetic force will be produced to make the rotor rotate.

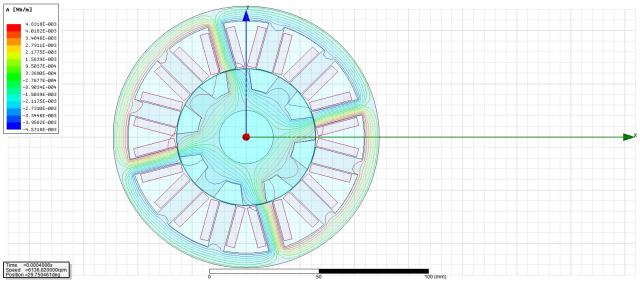

Fig.4 Distribution Map of Magnetic Force Line

Under the same conditions, the flux density distribution of the motor can be viewed, as shown in Fig. 4-14. The saturation degree of stator core can be obtained from the color in the figure. In the magnetic density contrast card in the upper left corner, red represents a high degree of magnetic saturation, while downward magnetic saturation decreases in turn. In the flux density distribution of the motor, the color is yellow, indicating that the flux density is not saturated, making full use of the stator core

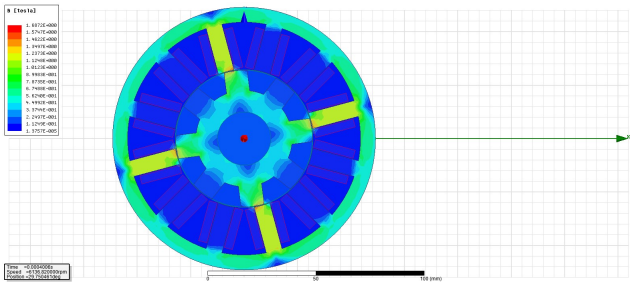

Fig.5 Flux Density Distribution Map

5. Ansys and results

In Ansoft electromagnetic simulation environment, the necessary parameters of the motor are input, and the motor model is created to simulate and analyze the SRM of two different structures. The winding self-inductance, mutual inductance, torque and winding current of two different SRM motors are compared. The results are as follows.

A. Comparison of winding self-inductance

The induction characteristic curves of two SRM motors are measured by simulation software as shown in Fig. 6.

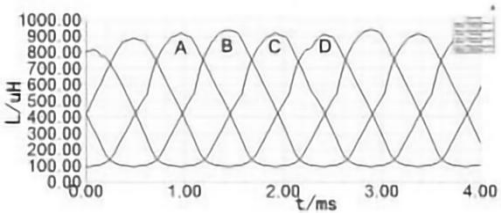

(a)8/6 poles self-perception

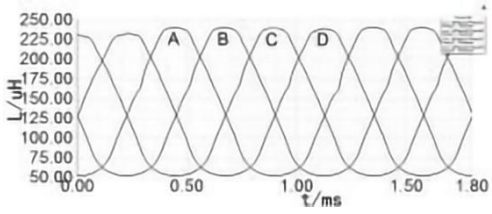

(b)16/12poles self-perception

Fig.6 Self-inductance characteristic curve

From Figure 6, it can be seen that the self-inductance variation law of each phase winding is basically the same, but the self-inductance amplitude is quite different. Taking A-phase winding as an example, the measured values of A-phase self-inductance parameters of two types of motors are shown in Table 2.

Tab.2 Comparison of two structural self-inductance parameters (A phase)

structure	L_{max}/ μH	L_{min}/ μH	L_{avg}/ μH	Rate of Self inductance
8/6	913.2	103.7	449.3	9.2
16/12	241.2	50.6	129.6	4.5

From the data in Table 2, it can be seen that the self-inductance values of two kinds of SRMs with the same parameters but different structures are quite different, and the maximum difference is nearly

500 H, and the minimum difference of self-inductance is also nearly 50 H. The change rate of the motor's torque and self-inductance is proportional, and the self-inductance change rate of the 8/6 pole motor is nearly twice that of the 16/12 pole motor.

The main reason for the difference of self-inductance is that the diameter of magnetic line is related to the structure of the motor itself. Specific analysis is as follows: Firstly, for the maximum self-inductance, the inductance depends on the flux and current. Compared with 16/12 and 8/6, the number of turns per pole and the extreme width of the former are reduced by twice. Theoretically, the maximum self-inductance of 16/12 is only1/4 of 8/6. This is verified by numerical simulation, as shown in Table 2. For the minimum self-inductance value, the theoretical analysis of 16/12 self-inductance value will also reduce, but no longer follow the 1/4 principle. The specific reason is shown in Figure 7. When the poles of stator and rotor are completely uncoupled, the air gap between stator and rotor is very large, resulting in a high reluctance value in the magnetic circuit and a low degree of magnetic saturation. The paths are almost the same, so there is little difference in self-inductance.

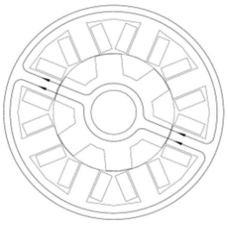

(a) 8/6 poles

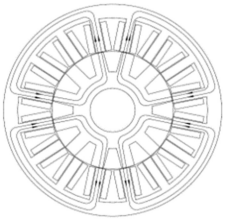

(b) 16/12 poles

Fig.7 Maximum self-inductance loop

B. Comparison of mutual inductance between windings

The excitation current will pass through the adjacent two-phase windings in turn when switched reluctance motor works normally, but during commutation, the adjacent two-phase windings will turn on at the same time, and the turn-on time will be close to 15 degrees of electrical angle, so there will be a mutual inductance in the adjacent two-phase conduction, while the non-adjacent two-phase conduction time is very short, then the mutual inductance value can be neglectable.

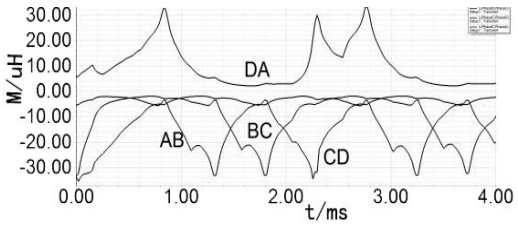

(a)8/6 poles mutual-perception

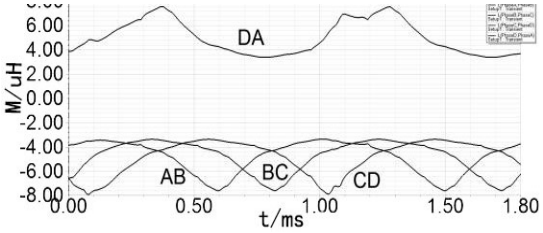

(b)16/12poles mutual-perception

Fig.8 Mutual inductance characteristic curve

Fig. 8 shows the mutual inductance characteristic curves of SRM motors with 8/6 poles and 16/12 poles of different magnetic poles. It can be seen that the mutual inductance curves of different structures are quite different and irregular. In terms of numerical value, the mutual inductance of SRM motors with different structures differs greatly, and there are negative values. In order to analyze the influence of mutual inductance on self inductance more clearly, the mutual inductance of AB phase and a phase of SRM with two different structures are compared, as shown in Table 3. Mmax represents maximum mutual inductance, Mmin represents minimum mutual inductance and Mavg represents average mutual inductance.

Tab.3 Comparison of two structural mutual inductance parameters (AB phase)

structure	Mutual inductance/μH			Self inductance of A phase/μH		
	M_{max}	M_{min}	M_{avg}	L_{max}	L_{min}	L_{avg}
8/6	31.8	2.1	9.5	913.2	103.7	449.3
16/12	7.6	3.1	4.7	241.2	50.6	129.6

As shown in Table 3, the mutual inductance values of SRM with two structures are quite different. For the average mutual inductance, 8/6 pole motor is twice that of 16/12 motor, and the average of the former is 2.16% of the average inductance value, while the average of the latter is about 4% of the average self-inductance value. For the maximum mutual inductance, the 8/6 pole SRM is four times as much as the 16/12 pole SRM, while the minimum mutual inductance has little difference between the two motors.

C. Comparison of Torque and Pulse Coefficient

Torque and ripple coefficient are two important parameters to measure motor performance. The bigger the torque, the stronger the motor's function force and the smaller the torque, the lower the efficiency of the motor and even the problem of no animal body will occur. Therefore, the size of the torque is of great significance to the determination and control of the load on the transmission shaft, the strength design of the working parts of the transmission system and the selection of the capacity of the prime mover. Torque ripple coefficient also seriously affects the performance of the motor. The larger the ripple coefficient, the greater the noise of the motor. Considering the optimal design of the motor, it is hoped that the torque of the motor will be large and the ripple coefficient will be small. Using electromagnetic simulation software, two SRM motors with different structures are simulated numerically, and the torque characteristic curves of the two motors are obtained as shown in the figure.

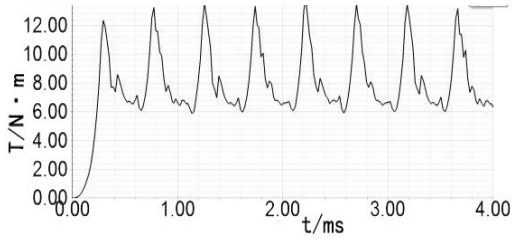

(a)8/6 poles torque

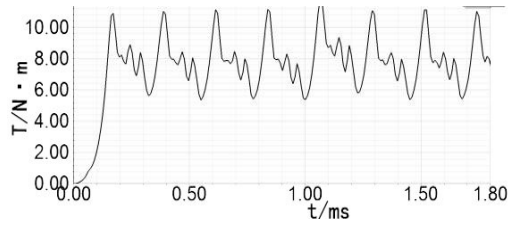

(b)16/12poles torque

Fig.9 Four-phase 8/6 pole and four-phase 16/12 pole SRM torque curve

Fig. 9 shows that the average torque of 8/6 pole SRM is about 8.21N.m, and the torque is between 5.83N.m-12.02N.m. The average pole torque of 16/12 pole SRM is about 7.96N.m, and it is between 5.87N.m-11.85N.m. Overall, there is little difference between the two types of motors. The torque performance of 8/6 pole motor is slightly higher than that of 16/12 pole motor.

The ripple coefficient of motor torque is correlated with the difference of the amplitude of the torque. The bigger the difference of the amplitude of the torque, the bigger the motor ripple and the more serious the corresponding motor noise. Fig. 5 shows that the maximum and minimum difference of 8/6 poles is about 7.19 N. m, and the difference of 16/12 poles is about 5.74 N. M. The difference of the magnitude of the torque is caused by the different proportion of the overlap area between the stator and rotor of the two motors. The higher the proportion of the overlap area, the smaller the difference of the magnitude of the torque and the corresponding reduction of the ripple coefficient, but the resulting reduction of the torque. Therefore, the pulsation coefficient of 16/12 pole SRM motor is smaller than that of 8/6 pole SRM, and the noise performance is improved, but the torque is also reduced. It can be used in occasions where the noise requirement is high and the dynamic performance requirement is not high.

D. Comparison of winding currents

The current characteristic curves of the stator windings of two SRM structures are further investigated, as shown in Fig. 10. As can be seen from Figure 6, the current trends of 8/6 pole SRM and 16/12 pole SRM windings are basically the same, but the current amplitude and average value of 8/6 pole SRM are obviously lower than that of 16/12 pole SRM. The smaller the current value is, the better the voltage-ampere capacity of the switch is.

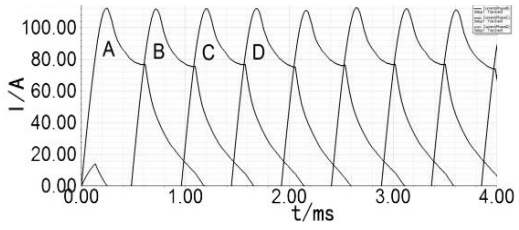

(a)8/6 winding current characteristic

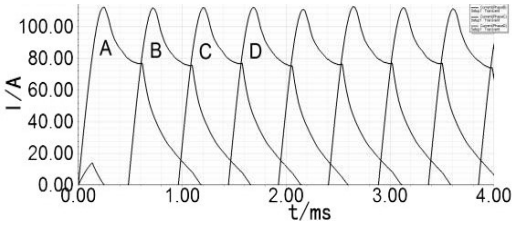

(b)16/12 winding current characteristic

Fig.10 Winding current characteristic curve

6. Conculsions

In this paper, two kinds of 8/6 pole and 16/12 pole SRMs with the same parameters and different stator and rotor structures are compared and analyzed based on Anosoft electromagnetic simulation software, and the following conclusions are drawn:

1) The difference of magnetic pole structure distribution and parameter setting leads to the difference of self-inductance between the two SRM motors. Compared with 16/12 poles, the maximum self-inductance of 8/6 pole SRM differs greatly, while the minimum self-inductance differs slightly, and the self-inductance of the former varies more than that of the latter. However, the self-inductance variation law of the two motors is basically the same.

2) The mutual inductance of SRM with two different structures will occur during commutation. The mutual inductance characteristic curves of SRM with different pole structures have no regular scientific research, and the mutual inductance of 8/6 poles affects the self-inductance less than 16/12 pole structure.

3) The difference of the magnetic pole structure results in the difference of the ratio coefficient of overlap area between stator and rotor. Compared with the 16/12 pole motor and the 8/6 pole motor, the difference of the torque is not significant. The numerical value of the torque is slightly lower than the latter, but the fluctuation coefficient is also reduced correspondingly, which is beneficial to the noise control of the motor.

4) Compared with 16/12-pole SRM, the winding current curve of 8/6-pole SRM tends to be consistent, and the current amplitude and average value of 8/6-pole SRM are obviously lower than that of 16/12-pole SRM. The smaller the current value is, the better the voltage-ampere capacity of the switch is, and the longer the service life of the switch is.

In summary, the different pole structures of stator and rotor will affect the performance of SRM to a certain extent. The above research results lay a foundation for the further development of the structure design of SRM motor, the improvement of torque, the reduction of torque ripple, the reduction of motor noise and other motor optimization design.

References

[1] Vijayakumar K, Karthikeyan R, Paramasivam S, et al.Switched reluctance motor modelling, design, simulation, and analysis: a comprehensive review[J]. IEEE Transactions on Magnetics, 2008, 44(12): 4605-4617.

[2] Li W, Sheng M, Huo F. Optimal design and finite element analysis of switched reluctance motor for electric vehicles[C]. IEEE VPPC, 2008: 1-5.

[3] Li W, Sheng M, Huo F. Optimal design and finite element analysis of switched reluctance motor for electric vehicles[C]. IEEE VPPC, 2008: 1-5.

[4] Takemoto M，ChIba A，Akagi H，et al．Radial force and torque of a bearing less switched reluctance motor operating in a region of magnetic saturation［J］. IEEE Transactions on Industry Application，2004，40(1) : 103－112．

[5] Vijayakumar K, Karthikeyan R, Paramasivam S, et al.Switched reluctance motor modelling, design, simulation, and analysis: a comprehensive review[J]. IEEE Transactions on Magnetics, 2008, 44(12): 4605-4617
[6] Zhu Yueying, Zhao Guifan, Yang Nal. Design and optimization for switched reluctance motor drive system in Electric vehicles[J]. Transactions of China Electrotechnical Society, 2014, 29(11): 88-98.
[7] Bostanci E, Moallem M, Parsapour A, et al. Opportunities and challenges of switched reluctance motor drives for electric propulsion: a comparative study[J]. IEEE Transactions on Transportation Electrification, 2017, 3(1): 58-75.
[8] Sozer Y, Husain I, Torrey D A. Guidance in selecting advanced control techniques for switched reluctance machine drives in emerging applications[J]. IEEE Transactions on Industry Applications, 2015, 51(6): 4505-4514.
[9] Wu Hongxing, Sun Qingjie, Huang Yuping, et al. Review of method for switched reluctance motor nonlinear modeling[J]. Micromotors, 2014, 47(5): 83-92.
[10] Torrey D A, Lang J H. Modelling a nonlinear variable reluctance motor drive[J]. IEE Proceedings -Electric Power Applications, 1990, 137(5): 314-326.
[11] Mihic D S, Terzic M V, Vukosavis S N. A new nonlinear analytical model of the SRM with included multiphase coupling [J]. IEEE Transactions on Energy Conversion, 2017, 32(4): 1322-1334.
[12] Song S J, Ge L F, Ma S J, et al. Accurate measurement and detailed evaluation of static electromagnetic characteristics of switched reluctance machines[J], IEEE Transactions on Instrumentation and Measurement, 2015, 64(3): 704-714.
[13] Shen L, Wu J H, Yang S Y, et al. Fast flux linkage measurement for switched reluctance motors excluding rotor clamping devices and rotor position sensors[J]. IEEE Transactions on Instrumentation and Measurement, 2013, 62(1): 185-191.
[14] Wang L X, Mendel J M. Generating fuzzy rules by learning from examples [J]. IEEE Transactions on Systems, Man, and Cybernetics, 1992, 22(6):
[15] Chen B, Liu X P, Ge S S, et al. Adaptive fuzzy control of a class of nonlinear systems by fuzzy approximation approach[J]. IEEE Transactions on Fuzzy Systems, 2012, 20(6): 1012-1021.

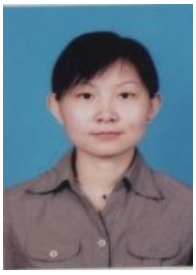

Ye Rong is currently pursuing her PhD study at Army Engineering University of PLA, Shijiazhuang, China. She obtained her BS degree from Xinyang University of Normal, China in 2007 and her MS degree from Hebei University of Normal, China in 2018. Her main field now is the study of magnetic properties of electrical materials.

Qingyi Kong is Doctor of Engineering. The research direction of the post-doctoral program of the Army Engineering University is the new technology of engineering electromagnetic field.

Wenda Qi is Doctor of Mechanical and Electronic Engineering, mainly engaged in electromagnetic emission technology, magnetohydrodynamics research.

Chao Li is studying in Hebei Vocational and Technical College of communications, majoring in railway power supply technology, mainly in the field of intelligent vehicle guidance, switched reluctance motor optimization design.

Huan Wu is studying in Hebei Transportation Vocational and technical college, majored in railway power supply technology and strawberry, mainly in the field of intelligent vehicle guidance, switched reluctance motor optimization design.